



LAWRENCE
LIVERMORE
NATIONAL
LABORATORY

Impact of Long-Range Dust Transport on Northern California in Spring 2002

P. Cameron-Smith, D. Bergmann, C. Chuang, G.
Bench, S. Cliff, P. Kelly, K. Perry, T. VanCuren

February 10, 2005

Disclaimer

This document was prepared as an account of work sponsored by an agency of the United States Government. Neither the United States Government nor the University of California nor any of their employees, makes any warranty, express or implied, or assumes any legal liability or responsibility for the accuracy, completeness, or usefulness of any information, apparatus, product, or process disclosed, or represents that its use would not infringe privately owned rights. Reference herein to any specific commercial product, process, or service by trade name, trademark, manufacturer, or otherwise, does not necessarily constitute or imply its endorsement, recommendation, or favoring by the United States Government or the University of California. The views and opinions of authors expressed herein do not necessarily state or reflect those of the United States Government or the University of California, and shall not be used for advertising or product endorsement purposes.

This work was performed under the auspices of the U.S. Department of Energy by University of California, Lawrence Livermore National Laboratory under Contract W-7405-Eng-48.

Impact of Long-Range Dust Transport on Northern California in Spring 2002

Philip Cameron-Smith, Dan Bergmann, Cathy Chuang, Graham Bench (LLNL),
Steve Cliff, Peter Kelly (UC Davis),
Kevin Perry (U.Utah), Tony VanCuren (Cal. ARB)

1 Abstract

It has been well documented that spectacular dust storms in Asia (*eg* the events in 1998 and 2001) can affect the USA through long-range transport of dust across the Pacific. However, our observations and modeling show that the majority of dust at sites in Lassen National Park and Trinity Alps (Northern California) in spring 2002 (a year with no spectacular Asian dust events) is still from long-range intercontinental transport across the Pacific.

We implemented the interactive dust emission algorithm of Ginoux et al. (2004) into the LLNL 3-D global atmospheric chemistry and aerosol transport model (IMPACT), then ran the model using a separate tracer for each dust emission region, using hi-resolution (1x1 degree) meteorological data from the NASA GMAO GEOS-3 assimilation system for 2001 and 2002. We also experimentally analyzed size- and time-resolved aerosol samples at Lassen National Park and Trinity Alps in the spring of 2002, which were taken as part of NOAA's ITCT 2k2 measurement campaign.

The model-predicted time-series of soil dust over Northern California agrees remarkably well with our measurements, with a strong temporal correlation between the observations and intercontinental transport of dust across the Pacific in the model. Hence, we conclude that the majority of dust we sampled in Northern California in spring 2002, with aerodynamic diameters of 0.56–5 microns, is from long-range intercontinental transport across the Pacific. The strong correlations also strongly validate atmospheric transport in the IMPACT model over the Northern Pacific in spring.

2 Introduction

Airborne aerosols cause adverse health effects; degrade visibility; affect the climate by reflecting sunlight directly and indirectly (through interactions with clouds); and supply nutrients that fertilize the oceans. Significant amounts of airborne mineral dust are known to blow to California across the Pacific Ocean from after spectacular dust storms in Asia, such as the events in 1998 and 2001. Since mineral dust can cross the Pacific, other aerosols presumably do too (*eg*, sulfates, nitrates, organic matter, and black carbon). Much of the mineral dust produced in Asia comes from China, which has suffered land degradation because of excessive agricultural use.

The size of aerosols is often critical to their transport and impact. For example, aerosols larger than about a micron tend to settle out of the atmosphere; aerosols smaller than 10 microns can penetrate deep into the lungs and must be cleared from the body through the cardio-vascular system; and the scattering of sunlight is strongly dependent on the size of the aerosols relative to the wavelength of the light. Hence, a full understanding of the impact of aerosols requires size-resolved treatment of aerosols.

The 2002 Intercontinental Transport and Chemical Transformation study (ITCT-2K2) [<http://www.al.noaa.gov/ITCT/2k2/>] was a major research activity of the International Global Atmospheric Chemistry (IGAC) [<http://www.igac.noaa.gov/>] program addressing the tropospheric chemistry and transport of ozone, fine particles and other chemically active greenhouse-compounds. The 2002 field study focused on transport across the North Pacific Ocean to North America, using a heavily instrumented primary ground site at Trinidad Head, CA supplemented by aircraft sampling over coastal North America and adjacent areas of the Pacific Ocean. During the ITCT-2K2 sampling period (mid-April through May, 2002) we conducted a continuous aerosol monitoring program using 8-Stage Davis Rotating Uniform size-cut Monitor (8-DRUM) impactors at Trinidad Head, CA, Trinity Alps, CA, and Lassen Volcanic National Park, CA, and fine particle (<2.5 micrometer) 3-stage DRUM samplers at Crater Lake National Park, OR, and White Mountain, CA.

3 Model Description

3.1 IMPACT model

The LLNL-IMPACT model is a 3D off-line chemistry & aerosol transport model that predicts concentrations in the coupled troposphere and stratosphere. The IMPACT model uses the operator splitting technique for emissions, advection, diffusion, convection, deposition, gravitational settling, photolysis, and chemistry. Advection is based on a version of the Lin-Rood, 1996, scheme, and uses a pressure-fixer scheme to ensure conservation of tracer mass [Rotman et al., 2004]. Diffusion is based on the implicit scheme of Walton et al. [1988]. Convection is based on the CONVTRANS algorithm of

Rasch et al. [1997]. Wet-deposition of species is based on their Henry's law coefficient, and is handled separately for scavenging within convective updrafts, the rest of the convective system, and stratiform clouds. Our scheme is based on Giorgi and Chameides [1986], Balkanski et al. [1993] Mari et al. [2000] and Liu et al. [2001]. Dry-deposition uses the resistances in series approach based on Wesely et al. [1985, 1989] and Wang et al. [1998]. Gravitational settling of particles is based on Seinfeld and Pandis [1998]. The 2000 emissions used for this work came from Granier et al. [2004], except for NO_x from lightning and aircraft, and CH₄, for which we used our standard 1990s emissions [Rotman et al., 2004] for both 2000 and 2100.

In order to compare our model results to observations, we modified IMPACT to use meteorological fields from the NASA GMAO GEOS-3 meteorological data assimilation system, which provides meteorological fields that are consistent with observations from satellites and in-situ measurement sites. The met-data is available every six hours.

In order to minimize the mismatch in scale between IMPACT (a global model) and our observations (point samples), we also increased the horizontal resolution of IMPACT to match the 1x1 degree resolution of the GEOS-3 met-data, which is more than double the previous state-of-the-art resolution (2x2.5 degrees). Unfortunately, this increase in resolution significantly increased the computational overhead, which scales as the fourth power of resolution. In large part this is because one must reduce the timestep in order to satisfy the Courant condition. In this case, we cut the primary timestep (for operator splitting) in half to 15 min, and then sub-cycled the advection operator to avoid the current-limit near the poles.

3.2 Dust emission

The emission of dust with the IMPACT model was done using the algorithm of Ginoux *et al.*, 2004. The temporally and spatially varying dust emission term is calculated from both an emission source function which varies with location, and a term dependant on the local 10 meter wind speed and soil moisture (provided by the GEOS-3 assimilated meteorological data). The emission was calculated using an effective radius for four different size bins (Table 1) where the mass distribution within each size bin was assumed to be constant with radius ($dM/dr = \text{const}$) for all but the smallest size bin, which mass distribution is assumed to be constant with log-radius ($dM/d\ln r = \text{const}$). Also included in the table are the corresponding range of aerodynamic diameters (diameter of a particle with unit density that has the same settling velocity) which will be used when comparing model results to measurements. A particle density of 2.65 g/cm³ was used for all for size bins.

Size Bin	Radius (μm)	Emission Radius(μm)	Aerodynamic Diameter (μm)	Total emitted (Tg)
1	0.1 – 1.0	0.63	0.40 – 3.4	216
2	1.0 – 3.0	2.0	3.4 – 9.8	1391
3	3.0 – 6.0	4.5	9.8 – 19.6	747
4	6.0 – 10.0	8.0	19.6 – 32.6	769

Table 1. Size bins used within model.

Using the meteorology from GEOS-3 for July 2001 through June 2002 at a horizontal resolution of 1x1 degrees 3123 Tg of dust were emitted (1607 Tg for dust with aerodynamic diameters less than 9.8 micron) which is within the range of values for total annual emission from other models (for publications since 2001, the range of emissions is 1000-2150 Tg/year for particles with aerodynamic diameter less than 10 microns; Zender, 2004). This was without rescaling or retuning any of the factors from Ginoux.

Figure 1 shows the total annual dust emission for all 4 dust sizes. The emission within the model was divided into 6 regions (Gobi, Takla Makan, Middle East, Sahara, North America, and Southern Hemisphere) and each of the 4 dust sizes from each of the 6 regions (24 total species) was tracked separately within the model.

Total Dust source calculated within IMPACT using GEOS3

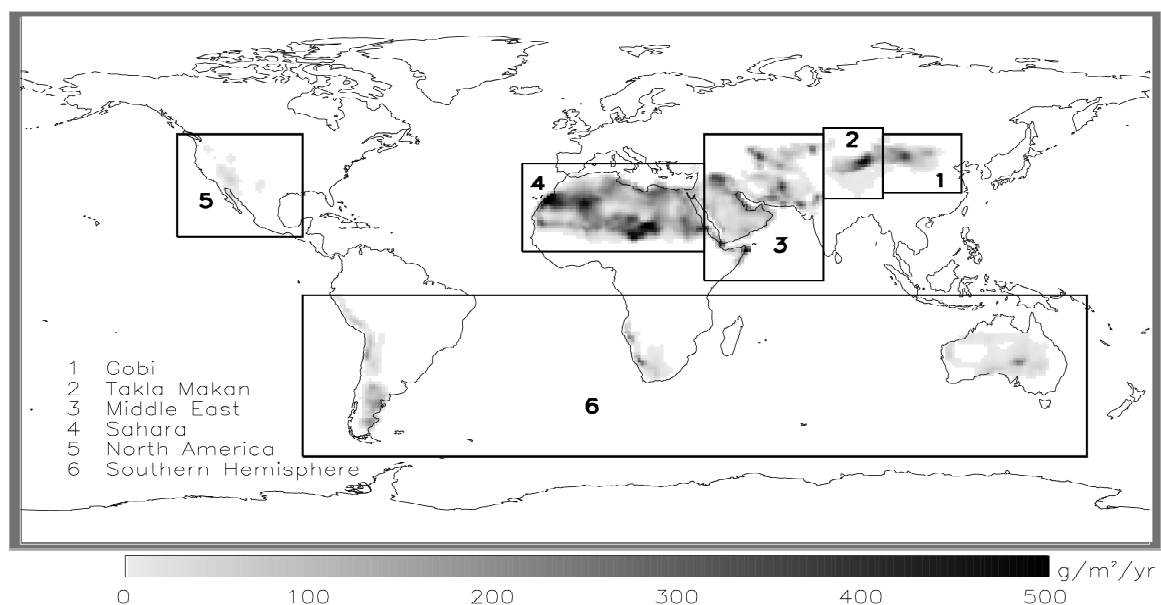


Figure 1 Total annual dust emission for all 4 dust sizes combined. The regions are 1) Gobi, 2) Takla Makan, 3) Middle East, 4) Sahara, 5) North America, and 6) Southern Hemisphere. The dust from each of the 6 regions, in each of 4 size bins (24 total species) was tracked separately within the model.

4 Observations

4.1 Description of Samplers

The 8-Stage Rotating DRUM Impactor Sampler (8-DRUM) used in this study is a cascade impactor based on the basic design of Lundgren [1967], and evolved from the original DRUM impactor as described by Raabe *et al.* [1988]. The sampler as configured for the present work operated at 16.7 liters per minute. The samplers located at the Trinity and Trinidad Head sites were coupled to a 10 μm cutpoint cyclone (“PM₁₀”) inlet; the sampler at the Lassen site used only a protective rain shield with an undefined (ca. 15 μm) primary cut. While the sampler for this work uses a slightly modified orifice design, impactor theory predicts similar efficiency for particle collection and robust size-cut determination as reported in Raabe *et al.* [1988]. The aerosol sample for each stage is deposited onto a rotating drum faced with a removable greased Mylar impaction surface. As the drum rotates a continuous aerosol sample is laid down along the direction of rotation with density varying along the length of the Mylar strip in proportion to the aerosol collected as the drum rotates. By replacing the circular jets of the original DRUM with slits, the aerosol deposit is made uniform crosswise to the direction of rotation and the total deposit is spread over a known area per unit time (*Bench et al.*, 2002). With the drums for all stages of the impactor geared together, coincident samples are collected on all eight stages. Analysis using a narrow X-ray beam scanned along each strip produces X-ray fluorescence elemental analyses with time resolution proportional to the ratio of drum surface speed divided by the beam width. For ITCT-2K2, the samplers were configured to provide a 42-day continuous record in 8 size bins (10-5, 5-2.5, 2.5-1.15, 1.15-0.75, 0.75-0.56, 0.56-0.34, 0.34-0.26, 0.26-0.09 micrometers aerodynamic diameter) analyzable in 3-hr time steps. Note that the stages are numbered from largest to smallest, the opposite direction to the model convention.

4.2 Deployment of Samplers

The ITCT-2K2 experimental plan used a heavily instrumented primary ground site on the Northern California coast at Trinidad Head, CA supplemented by aircraft missions over the eastern Pacific Ocean. For our study the Trinidad Head site was supplemented with nearby mountain sites. The mountain monitoring was suggested by the results of published Asian dust analyses which showed that coastal sites in California may miss Asian transport events due to the strong, persistent marine inversion common along the west coast of North America [*VanCuren and Cahill*, 2002] as well as from our preliminary results from the Aerosol Characterization Experiment In Asia (ACE-Asia; <http://saga.pmel.noaa.gov/aceasia/>). The intent of the multi-site experiment was to use continuous data to explore novel aspects of trans-Pacific aerosol transport:

First, we proposed to evaluate the temporal variability of Asian impacts in western North America. Previous aerosol analyses [*VanCuren and Cahill*, 2002; *VanCuren*, 2003] showed strong and regular Asian impacts in this region, but the intermittent sampling on

which those reports were based could not support analyses of the frequency and duration of individual transport events, whereas continuous measurements permit direct observation of the temporal structure of trans-Pacific aerosol transport.

Second, we planned to examine the lower troposphere/marine boundary layer separation of trans-Pacific aerosol transport. Statistical analysis of intermittent sample data [VanCuren and Cahill, 2002] showed a strong vertical gradient of Asian impact along the Pacific coast of North America. Simultaneous monitoring at sea-level and elevated sites in the present study permits direct examination of this vertical zonation of Asian aerosols, allowing validation (or refutation) of the impression given by preliminary analysis of twice-weekly samples (VanCuren, 2003).

The third goal was determination of the temporal pattern of mixing states (local vs. Asian) of lower free-troposphere aerosols over the west coast of North America. Previous work [VanCuren, 2003] showed that the long-term composition of the aerosols at elevated sites in the study region is dominated by Asian materials. Continuous sampling for a period of several weeks provides a means to assess the temporal structure of the relative contributions of Asian and North American sources to the observed aerosol loading, and to determine whether the region's aerosols are generally a mixture of Asian and local materials, or if air masses associated with the Asian and North American aerosols remain distinct within a regime of alternating Asian and local influences.

The mountain sampling sites themselves were chosen because they are part of the IMPROVE network [<http://vista.cira.colostate.edu/improve/>; Cahill and Wakabayashi, 1993]. IMPROVE sites offered power, space, and security to operate the 8- DRUM samplers unattended, as well as overlap with the IMPROVE long term aerosol records.

The ITCT-2K2 primary ground site was at sea level at Trinidad Head (41.05N, 124.15W). The IMPROVE Trinity Alps site is located at Pettijohn Mountain in the coast ranges (40.78N, 122.81W), elevation 1007 m, about 100 km east-southeast of Trinidad Head. The Lassen Volcanic National Park site is located at the Manzanita Lake Ranger Station on the north side of Mt. Lassen in the southern Cascade range (40.54N, 121.58W), elevation 1755 m, about 200 km east-southeast of Trinidad Head.

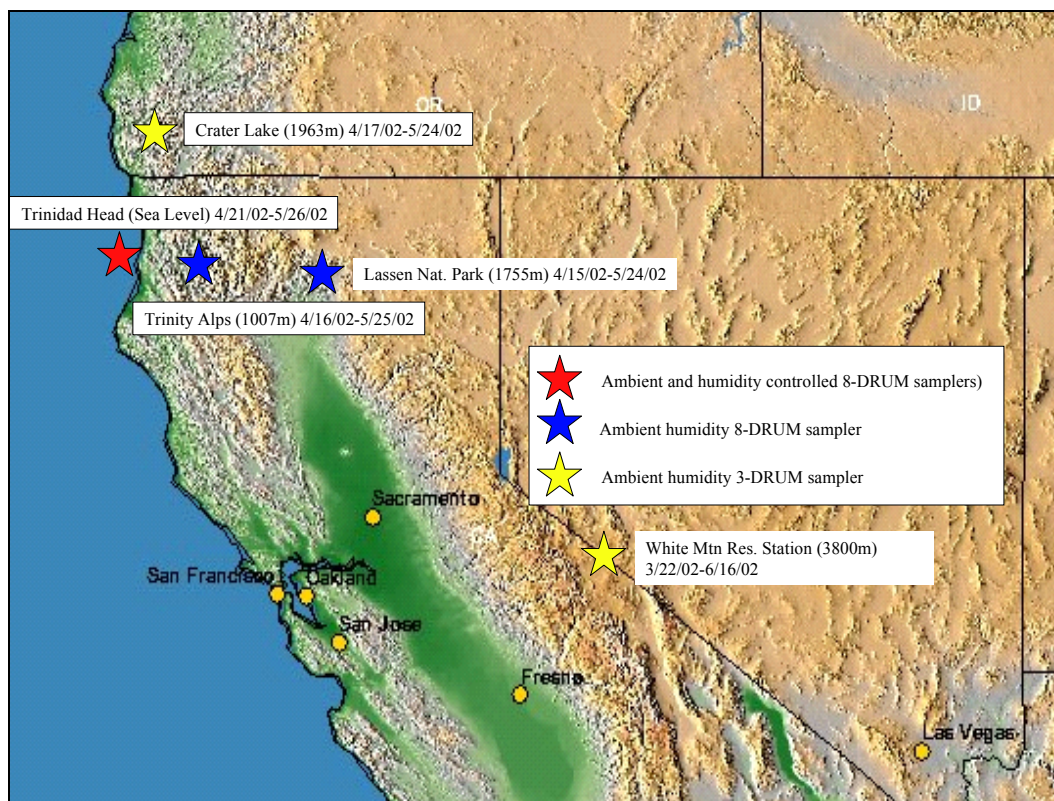


Figure 2 Our measurement sites during the ITCT-2k2 campaign, plus the altitudes and dates during which the samplers were active.

In this study, we focused on the measurements by 8-drum samplers since they have been better characterized than the 3-drum samplers, as well as resolving the aerosol size distribution more accurately. Unfortunately, although the Trinidad Head site was the best instrumented, with two 8-drum samplers and other supporting instruments, the Trinidad Head site was primarily influenced by the marine boundary layer, and almost no soil dust was observed. Hence, in this study we focused on the Lassen and Trinity Alps observations.

4.3 Analysis of Samples

Samples were analyzed by synchrotron X-ray fluorescence (S-XRF) [Knochel, 1989] using a broad-spectrum X-ray beam generated on beamline 10.3.1 at the Advanced Light Source (ALS) Lawrence Berkeley National Laboratory. The ALS S-XRF system is capable of detecting elements from Na to U (Perry et al. 2004).

The S-XRF analysis provided quantitative elemental data for approximately 28 elements in 8 size modes with 3-hour time resolution for the 6 week ITCT-2K2 campaign. Soil concentration is calculated from the assumed stoichiometric oxides of soil containing elements using the algorithm: $[SOIL] = 2.20[Al] + 2.49[Si] + 1.63[Ca] + 2.42[Fe] + 1.94[Ti]$ (Malm et al., 1994).

5 Model-Observation Comparison

We simulated the 18 month period from January 2001 through June 2002 using the IMPACT model described in section 3.1 at 1x1 degree resolution, with the soil emissions labeled by region as described in section 3.2. This covered the observations (spring 2002) with over a year of spin-up, which is ample since the lifetime of soil in the troposphere is days to weeks. From this run we output monthly mean concentrations and depositions for each soil size-bin and source region, plus more frequent snapshots of dust concentrations during the observation time-period. We also output a time-series of dust concentrations for each size-bin and source region over each of the measurement sites at every model time-step (15 min).

A time-series comparison of the measured soil concentrations against the modeled dust concentrations is shown in Figure 3 and Figure 4 for the Lassen and Trinity sites respectively. For these plots we compared the sum of size bins 1 & 2 from the model (0.1–3 micron radius; 0.4–9.8 micron aerodynamic diameters) with stages 2 to 5 of the drum sampler (aerodynamic diameters of 0.56–5 microns). In the model, bin 2 contains almost all the soil mass at the measurement sites. This is because the larger particles (bins 3 & 4) have larger settling velocities and fall out of the atmosphere closer to the source regions, while the smaller particles (bin 1) do not contain much mass because mass scales with the third power of radius. Hence, even though the bins in the model cover a slightly wider range of aerosol sizes than the measurements, the two ends of the distribution contribute little to the predicted aerosol mass.

For the drum samplers, we selected stages 2 to 5, which cover aerodynamic diameters of 0.56–5 microns. We ignored stage 1 because previous analysis has shown that the large particles it contains are typically from local dust sources (VanCuren, *et al.*, 2005). The upper limit of stage 1 is also less well defined than the other cut-offs. We ignored stages 6 to 8, which contain the smaller particles because previous experience has shown that they contain a lot of aerosols from combustion, which could contaminate the soil signature we were looking for.

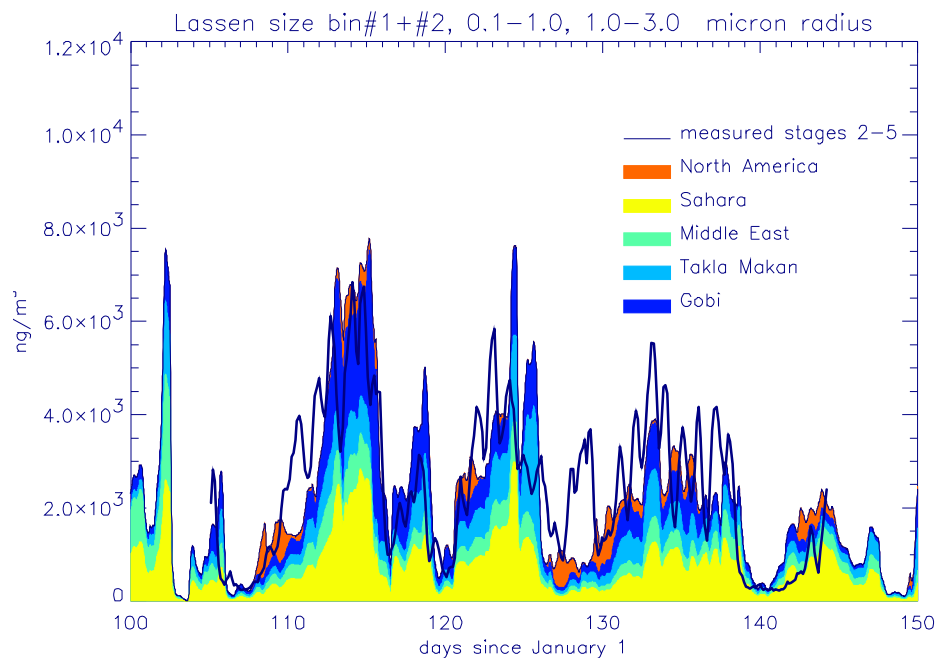


Figure 3 Time series comparison between aerosol concentrations measured at the Lassen site, and the dust from size bins 1 & 2 in the model (0.1-3 micron radius; 0.4 – 9.8 micron aerodynamic diameters) for the grid-box containing the measurement site at the altitude of the site. The concentrations from the different source regions in the model are stacked, so that the envelope of the model data is the total aerosol concentration from the model. Stages 2 to 5 of the drum sampler cover particles with aerodynamic diameters of 0.56-5 microns.

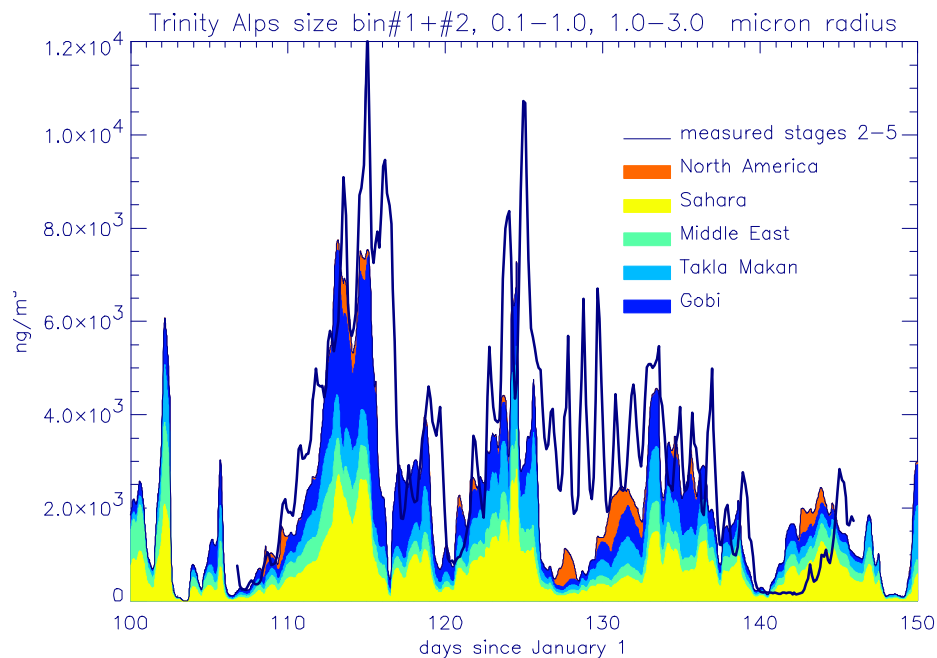


Figure 4 Same as Figure 3, but for the Trinity site.

There were no spectacular dust storms during this period, yet the measurements and the

model both show events lasting several days, with diurnal variability superimposed. A close comparison shows that the diurnal variability in the measurements and model are out of phase. This discrepancy is a result of the differing mechanisms by which the model and the real world bring the aerosols from the free troposphere down to the surface. In the model, air from the free troposphere is brought down to the surface through mixing in the boundary layer, which is most vigorous during the day. In contrast, these measurement sites, which are in mountainous regions, appear to be strongly affected by down-slope flow from the free troposphere at night (VanCuren, *et al.*, 2005).

To remove the diurnal variability and the attendant anti-correlation between the model and measurements, we convolved each time-series with a 24-hour top hat kernel. The resultant 24-hour running means are shown in Figure 5 and Figure 6.

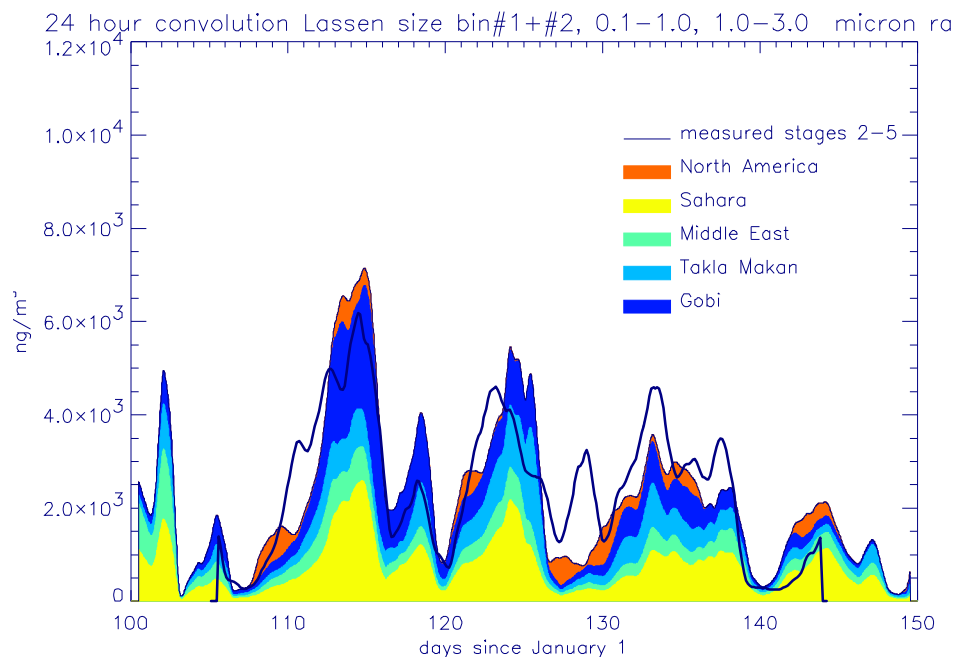


Figure 5 A 24-hour running mean of the time-series from Lassen shown in Figure 3.

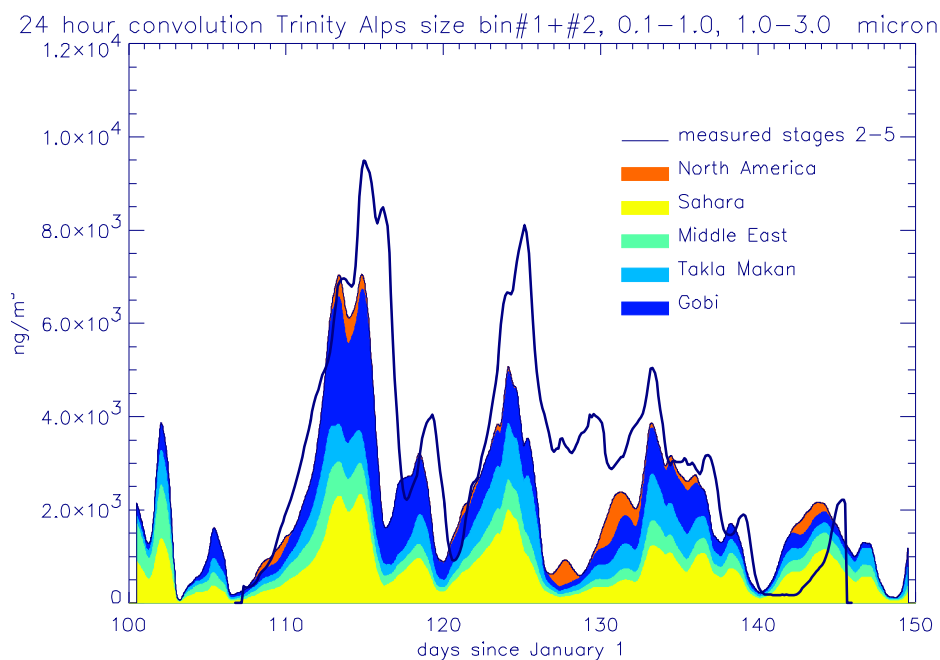


Figure 6 A 24-hour running mean of the time-series from Trinity Alps shown in Figure 4.

With the diurnal variability removed, the agreement between the timing, size, and duration of the episodic events can be seen more clearly. The remarkable agreement between the timing, shape, amplitude, and duration of the events was initially surprising to us, given (1) the disparate scales of the measurements and the model (meters versus 100 kilometers), (2) the fact that there was no model tuning or adjustment, (3) the total lack of any sources local to the measurement (within 100 km), and (4) the dependence of dust emission in the model to the assimilated wind-speed (to the third power) and soil moisture that are subject to the grid-scale of the assimilation model (100 km) and its parameterization of the relevant sub-gridscale processes. The reason for the remarkable agreement lies in the source of the measured soil particles.

The source of the measured soil particles is apparent when the soil from each source region in the model is correlated with the total observed soil, as shown in Figure 7 and Figure 8. All of the source regions, except the North American sources, are strongly correlated with the observed soil mass. The lack of correlation with the North American sources is presumably due to the prevailing westerly winds over the USA, which will generally blow soil from the main North American sources (see Figure 1) away from Northern California.

For each of the source regions, except North American, the standard least-squares straight line fits are reasonable fits to the data in Figure 7 and Figure 8, with intercepts near the origin. This indicates that the proportion of soil arriving at the measurement sites from each of the source regions is fairly consistent.

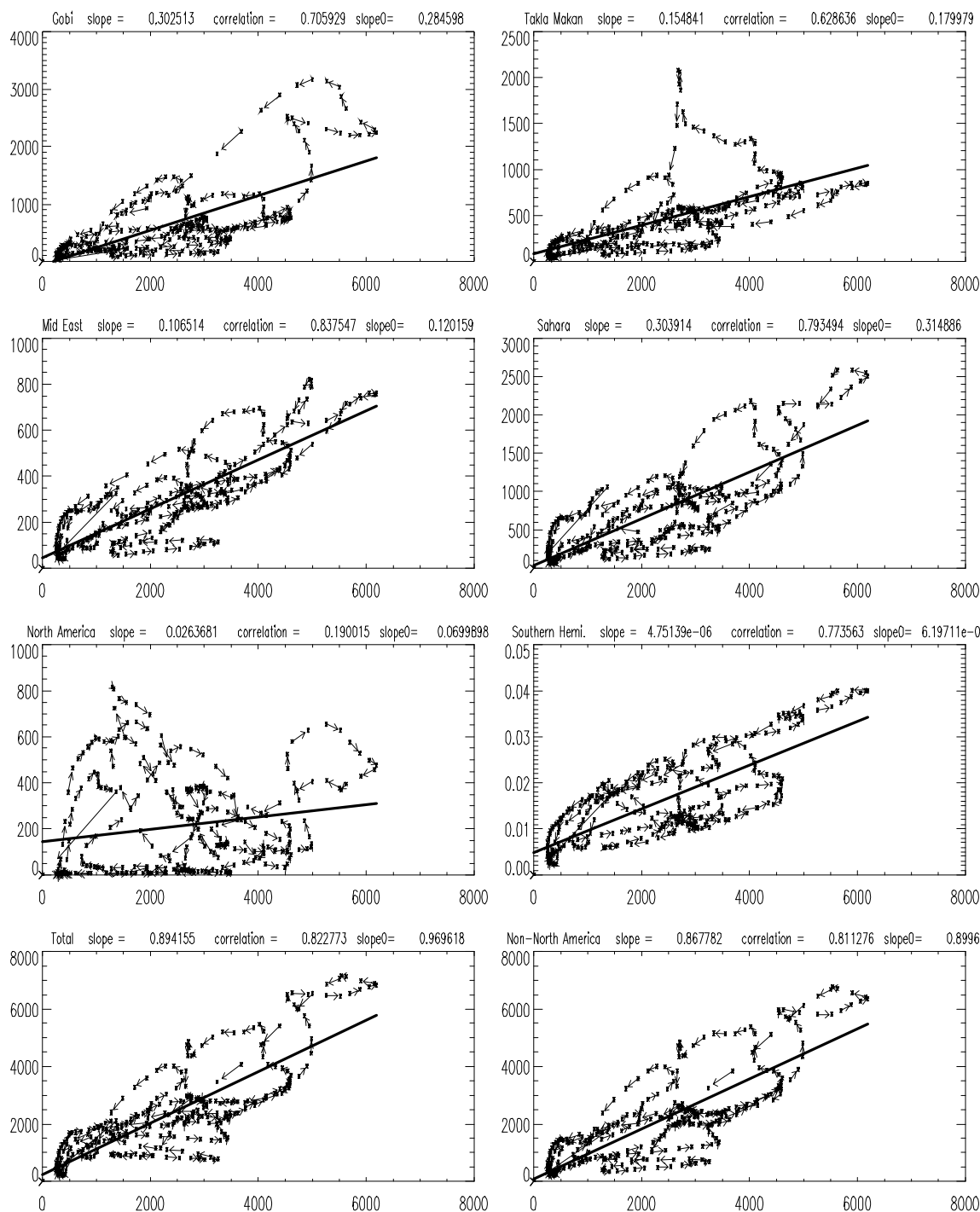


Figure 7 Scatter-plots, for the Lassen site, of the observed soil concentrations (x-axis) against the model predictions for 6 source regions plus the total of all the source regions, and the total of all regions except North America. The units of both axes are ng/m³. The straight line on each plot is the standard least squares best linear fit to the data (fitting both slope and intercept). The arrows indicate the flow of time among the data points. The correlation and two fitted slopes are given at the top of each plot. 'Slope' is the slope from least-squares fitting both slope and intercept, while 'Slope0' is the slope from a least-squares fit to a straight line constrained to go through the origin.

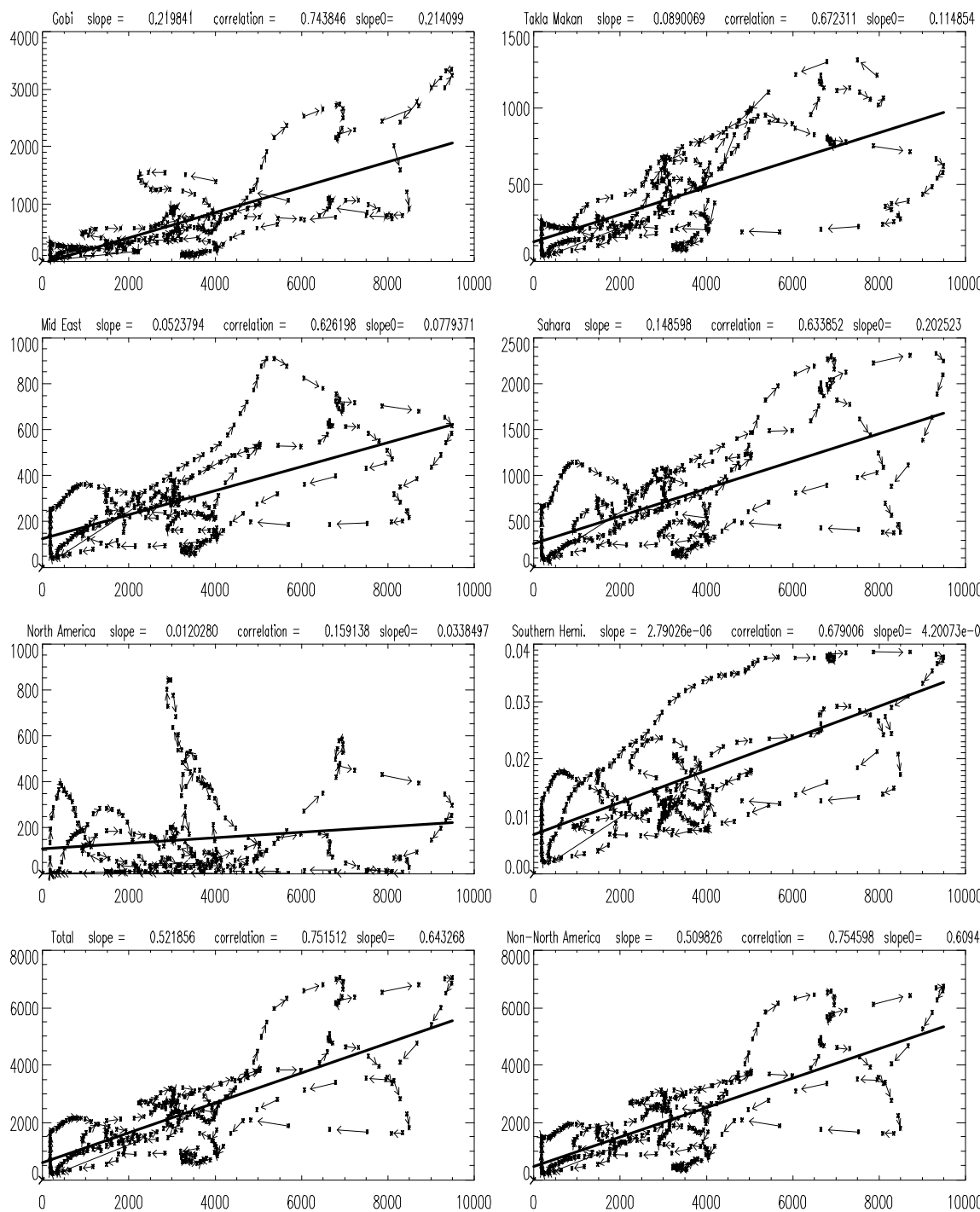


Figure 8 The same as Figure 7, but for the Trinity Alps site.

The contribution of any source of inert tracer to a measurement site is the emission from that source convolved with atmospheric transport. Thus, in order for the contribution from different sources regions to be correlated, either (1) the source emissions must be correlated (possibly with a time-lag) with identical atmospheric transport (with any required compensating time-lag), (2) the sources are all constant and the atmospheric

transport is essentially the same for all sources, or (3) there are compensating factors between the source emissions and the atmospheric transport which cancel.

Considering the third hypothesis, the chance of the source emissions and atmospheric transport conspiring to give the highly correlated results we see in the model when there are multiple source regions is so improbable that it can be easily dismissed. For the first hypothesis, sources being correlated by some sort of teleconnection, is easily tested in the model by looking at the time-series of emissions from each region, shown in

Figure 9.

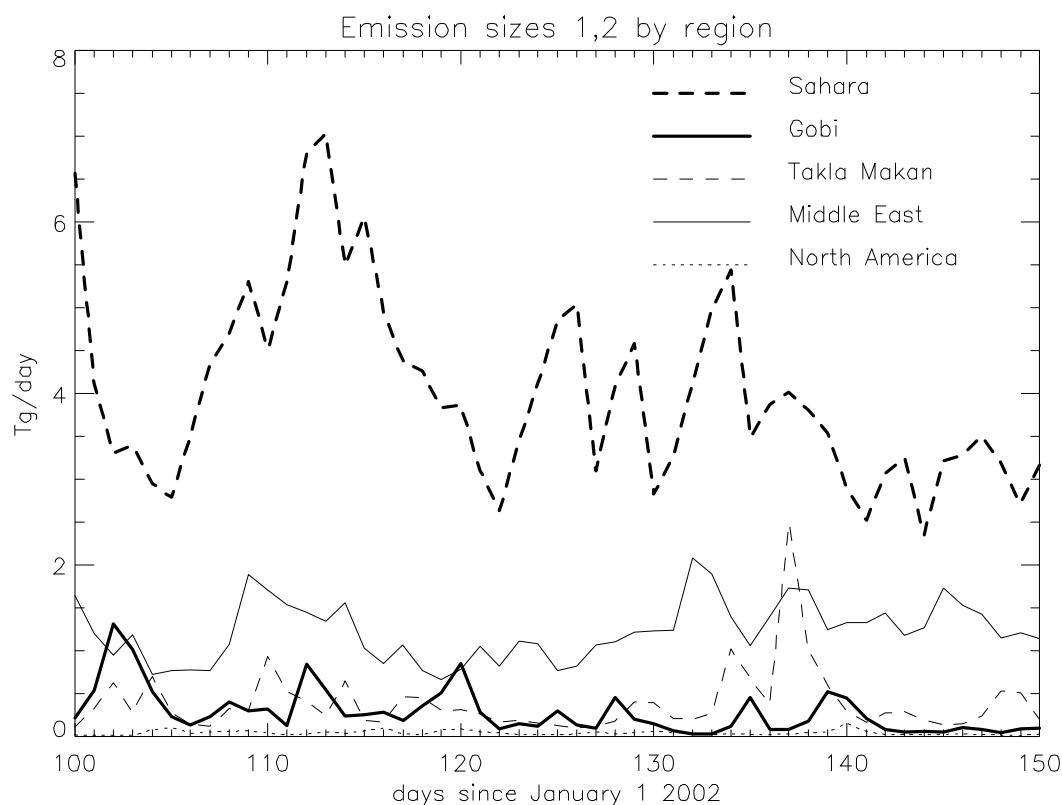


Figure 9 Time-series of daily-averaged soil emissions from each source region.

Since there is no obvious correlation between the emissions from the different regions, this leaves the second hypothesis, namely that the sources are constant and the atmospheric transport is the same for all of the sources. In support of this hypothesis,

Figure 9 shows that, while there is definitely variability in the emissions from each source region, the emissions are much more constant than the time-series at the measurements sites (in both model and measurements).

The second part of this hypothesis requires that the atmospheric transport be the same for each region. Visual examination of the 3D soil concentration fields in the model

indicates that (in this season at least) winds in the free troposphere consistently blow soil from parts of Africa over the Middle-East, and thence over China, mingling with soil lofted from the other source regions along the way. Thus, there is a large pool of mingled soil dust in the free troposphere over China, which then gets swept out over the Pacific by synoptic weather systems that carry the mingled soil dust around the Pacific. The dust that reaches the USA typically appears to travel via the northern Pacific over the Aleutian Islands, before heading south and descending over the western USA to impact the surface. Thus, the model indicates that the soil time-series we measured in Northern California is primarily dictated by the synoptic weather systems over the Pacific, which alternately bring to the measurement sites either clean Pacific air, or air from China that is laden with mingled soil from Africa, the Middle East, and China. The fact that soil from the southern hemisphere is also correlated, even though its concentration is negligible, indicates that the southern hemispheric soil that crosses the terminator similarly mingles with the other soils over China before being swept out by the synoptic weather systems. This result is consistent with the results of VanCuren *et al.* (2005) who showed that the elemental signature of the soil in these measurements is incompatible with a North American source.

Another implication of the good correlations between model and observations is that atmospheric transport must be well represented in the IMPCT model using the GMAO GEOS-3 meteorological fields (at least for the Pacific region in spring) in order for it to match the timing, shape, and width of the observed time-series. In order to test the timing more sensitively than simply looking at the time-series plots, we added arrows to show the order in time of the points in the scatter plots (Figure 7 and Figure 8). If the points circulate in a clockwise direction it implies that the model precedes the observations, whereas anti-clockwise circulation implies that the model lags the observations. Looking at the scatter plots in Figure 7 and Figure 8, the circulation is clearly anti-clockwise for Lassen and clockwise for Trinity. The reason for this difference is not clear, but since the sites are so close together in the model, it certainly argues against a systematic error in the model transport. Part of the answer may lie in the time-registration of the observations, since the start and end of the aerosol on the sample strips is determined by the first detection of signal, so the start-time of the observations is uncertain to the time-resolution of the measurements (3 hours).

To get a quantitative estimate of the relative contribution from each source region to the measurement sites, one can look to the slope of the fitted lines in Figure 7 and Figure 8. However, the slopes of the lines are affected by the non-zero intercepts. So, to get a better estimate we also calculated the least-squares slopes of lines that were constrained to go through the origin (slope = $\text{Sum}(x.y)/\text{Sum}(x^2)$). The slopes from these lines are given as 'slope0' on each scatter plot, and are tabulated in Table 2.

	Lassen (%)	Trinity (%)
Gobi	28	21
Takla Makan	18	11
Middle East	12	8
Sahara	31	20
North America	--	--
Southern Hemisphere	0	0
All Sources (Total)	97	64
Non-North American	90	61

Table 2 The contribution of each source region to the Lassen and Trinity sites determined from the slopes of the fitted lines constrained to go through the origin from Figure 7 and Figure 8. Note 1: the North American source is not correlated in time with the others, so its fitted slope cannot be interpreted as a consistent fraction. Note 2: the ‘All Sources’ and ‘Non-North American’ contributions were determined from the fits to those plots, rather than summing the individual slopes.

The model predicts the total soil concentration at the Lassen site surprisingly well, but clearly under-predicts the dust concentration at the Trinity site. The difference seems to be that there is a significant difference in the measured soil concentrations at the two sites, whereas the model predicts similar magnitudes at the two sites, which is not surprising because the two sites are in neighboring grid-cells in the model. Indeed, since the Lassen and Trinity sites are apparently sampling the same air-mass from the free troposphere, it is a little surprising that the observed amplitudes are so different. One possible explanation is that there is greater mixing of the free-tropospheric air with boundary layer air at the Lassen site, resulting in the lower soil concentrations.

One unfortunate aspect of the correlation between the contribution from the different source regions is that there are no times in the observations that can be ascribed to a single source, so there is no hope of identifying any elemental fingerprint from this dataset by itself to verify whether the contribution ratios predicted by the model are realistic. In principle, externally determined elemental signatures could be used, but with the mixture predicted to contain soils from several different regions it will be difficult to separate them all. Nonetheless, there does appear to be some information in the elemental ratios which merits further investigation.

6 Dust Budget for Continental USA

The model run described in section 5 also provided a 1-year simulation from July 2001 to June 2002 (after a 6 month spin-up) from which we calculated an intercontinental dust budget for the continental USA (48 states). The amount of dust deposited by the model over the region 28N-44N, 124W-72W in each month is given in Table 3 and Table 4.

	Gobi	Takla Makan	Middle East	Sahara	North America	Total
Jul-01	0.018	0.055	0.019	0.062	0.940	1.094
Aug-01	0.009	0.024	0.012	0.040	0.617	0.702
Sep-01	0.014	0.034	0.007	0.007	0.587	0.649
Oct-01	0.017	0.050	0.017	0.022	0.462	0.568
Nov-01	0.003	0.010	0.025	0.030	0.552	0.620
Dec-01	0.006	0.031	0.023	0.043	0.657	0.760
Jan-02	0.001	0.005	0.004	0.006	0.485	0.501
Feb-02	0.002	0.010	0.017	0.011	0.589	0.629
Mar-02	0.019	0.029	0.048	0.124	0.842	1.062
Apr-02	0.069	0.068	0.096	0.138	0.886	1.257
May-02	0.060	0.099	0.070	0.143	0.793	1.165
Jun-02	0.038	0.098	0.035	0.112	0.657	0.940
Total	0.256	0.513	0.373	0.738	8.067	9.947

Table 3 Dust deposited on the continental USA from all size bins.

	Gobi	Takla Makan	Middle East	Sahara	North America	Total
Jul-01	0.016	0.052	0.018	0.062	0.423	0.571
Aug-01	0.009	0.023	0.012	0.040	0.270	0.354
Sep-01	0.013	0.031	0.007	0.007	0.242	0.300
Oct-01	0.016	0.047	0.017	0.022	0.170	0.272
Nov-01	0.002	0.009	0.023	0.030	0.220	0.284
Dec-01	0.006	0.028	0.023	0.043	0.254	0.354
Jan-02	0.001	0.004	0.004	0.005	0.148	0.162
Feb-02	0.002	0.009	0.016	0.011	0.173	0.211
Mar-02	0.019	0.027	0.046	0.121	0.284	0.497
Apr-02	0.064	0.063	0.090	0.134	0.320	0.671
May-02	0.057	0.090	0.066	0.139	0.277	0.629
Jun-02	0.035	0.090	0.033	0.111	0.220	0.489
Total	0.240	0.473	0.355	0.725	3.001	4.794

Table 4 Dust deposited on the continental USA from size bins 1 & 2 (0.4-9.8 micron aerodynamic diameter).

Not surprisingly, soil dust emitted from North American dominates the deposition. The reason North American soil doesn't show up in our measurements discussed in section 5 is that the prevailing westerly winds blow North American soil to the east.

7 Conclusion

The remarkable agreement between the observations and the model indicates that the LLNL-IMPACT model, using GMAO GEOS-3 assimilated meteorology, is accurately simulating atmospheric transport over the Pacific in spring. The correlation to all the non-American sources also implies that airborne soil dust is dominated by sources outside the USA for mountain sites in the Northern California each spring.

Surprisingly, the model predicts that a significant fraction of the measured soil actually comes from Africa and the Middle East, in addition to China. Unfortunately, the African and Middle Eastern soil are so tightly correlated in time with soil from Asia, that it is impossible to determine from our current analyses of the observations the true contribution from each region.

The capability to model dust in the atmosphere will allow us to tackle other problems too, such as dust fertilization of oceans effecting ocean sequestration of CO₂, and the feedbacks between climate change and dust production.

8 Acknowledgements

This work was performed under the auspices of the U. S. Department of Energy (DOE) by the University of California, Lawrence Livermore National Laboratory (LLNL) under Contract No. W-7405-Eng-48. The project (03-ERD-021) was funded by the Laboratory Directed Research and Development Program at LLNL.

9 References

Balkanski, Y. J., D. J. Jacob, G. M. Gardner, W. C. Graustein, and K. K. Turekian (1993), "Transport and residence times of tropospheric aerosols inferred from a global three-dimensional simulation of ²¹⁰Pb", *J. Geophys. Res.*, 98, 20,573-20,586.

Bench, G., Grant, P., Ueda, D., Cliff, S., Perry, K., Cahill, T., The Use of STIM and PESA to Measure Profiles of Aerosol Mass and Hydrogen Content, Respectively, across Mylar Rotating Drum Impactor Samples, *Aerosol Science and Technology* 36: 642–651, 2002.

Cahill, T., and Wakabayashi, P., Compositional analysis of size-segregated aerosol samples. Chapter 7 in *Measurement Challenges in Atmospheric Chemistry*. Leonard Newman, Ed., *Am. Chem. Soc.*, 211-228, 1993.

DeMore, W. B., S. P. Sander, D. M. Golden, R. F. Hampson, M. J. Kurylo, C. J. Howard, A. R. Ravishankara, C. E. Kolb, and M. J. Molina (1997), "Chemical kinetics and photochemical data for use in stratospheric modeling", *JPL Publ.*, 97-4.

Douglass, A., R. B. Rood, S. R. Kawa, and D. J. Allen (1997), "A three dimensional simulation of the evolution of the middle latitude winter ozone in the middle stratosphere", *J. Geophys. Res.*, 102, 19,217-19,232.

Ginoux P, Prospero JM, Torres O, Chin M, "Long-term simulation of global dust distribution with the GOCART model: correlation with North Atlantic Oscillation", *ENVIRONMENTAL MODELLING & SOFTWARE*, 19 (2): 113-128, 2004.

Giorgi, F., and W. L. Chameides (1986), "Rainout lifetimes of highly soluble aerosols and gases as inferred from simulations with a general circulation model", *J. Geophys. Res.*, 91, 14,367-14,376.

Jacobson, M. A. (1995), "Computation of global photochemistry with SMVGEAR II", *Atmos. Environ.*, Part A, 29, 2541-2546.

Knochel, Basic Principles of XRF with Synchrotron Radiation, *2nd International Workshop on XRF and PIXE Applications in Life Science, Capri, Italy, 29-30 June, 1989*, World Scientific Publishing Co., Singapore, 1990.

Lin, S. J., and R. B. Rood (1996), "A fast flux form semi-Lagrangian transport scheme on the sphere", *Mon. Weather Rev.*, 124, 2046-2070.

Liu, H., D. J. Jacob, I. Bey, and R. M. Yantosca (2001), "Constraints from ²¹⁰Pb and ⁷Be on wet deposition and transport in a global three-dimensional chemical tracer model driven by assimilated meteorological fields", *J. Geophys. Res.*, 106, 12,109-12,128.

Lundgren, D. A., An Aerosol Sampler for Determination of Particle Concentration as a Function of Size and Time, *J. Air Poll. Cont. Assoc.* **17**, 225-229 (1967).

Lurmann, F. W., A. C. Lloyd, and R. Atkinson (1986), "A chemical mechanism for use in long-range transport/acid deposition computer modeling", *J. Geophys. Res.*, 91, 10,905-10,936.

Malm, W.C., J.F. Sisler, D. Huffman, R.A. Eldred, and T.A. Cahill. Spatial and seasonal trends in particle concentration and optical extinction in the United States. *Journal of Geophysical Research*, VOL. 99, No. D1, 1347-1370, 1994.

Mari, C., D. J. Jacob, and P. Bechtold (2000), "Transport and scavenging of soluble gases in a deep convective cloud", *J. Geophys. Res.*, 105, 22,255-22,267.

Perry K. D., S. S. Cliff, M. P. Jimenez-Cruz (2004), Evidence for hygroscopic mineral dust particles from the Intercontinental Transport and Chemical Transformation Experiment, *J. Geophys. Res.*, 109, D23S28, doi:10.1029/2004JD004979.

Raabe, O.G., D.A. Braaten, R.L. Axelbaum, S.V. Teague, and T.A. Cahill, Calibration Studies of the DRUM Impactor, *J. Aerosol Sci.* v. 19, p 183-195, 1988.

Rasch, P. J., N. M. Mahowald, and B. E. Eaton (1997), "Representation of transport, convection, and the hydrological cycle in chemical transport models: Implication for the modeling of short-lived and soluble species", *J. Geophys. Res.*, 102, 28,127-28,138.

"IMPACT, the LLNL 3-D global atmospheric chemical transport model for the combined troposphere and stratosphere: Model description and analysis of ozone and other trace gases", D. A. Rotman, C. S. Atherton, D. J. Bergmann, P. J. Cameron-Smith, C. C. Chuang, P. S. Connell, J. E. Dignon, A. Franz, K. E. Grant, D. E. Kinnison, C. R. Molenkamp, D. D. Proctor, and J. R. Tannahill, *J. GEOPHYS. RES.*, VOL. 109, D04303, doi:10.1029/2002JD003155, 2004.

Sander, S. P., et al. (2000), "Chemical kinetics and photochemical data for use in stratospheric modeling: Supplement to Evaluation 12: Update of key reactions", Evaluation 13, *JPL Publ.*, 00-003.

Seinfeld, J. H., and S. N. Pandis (1998), "Atmospheric Chemistry and Physics", John Wiley, New York.

VanCuren, R. and Cahill, T., Asian aerosols in North America: Frequency and concentration of fine dust, *J. Geophys. Res.* 107(D24), doi:10.1029/2002JD002204, 28 December 2002.

VanCuren, R., Asian aerosols in North America: Extracting the chemical composition and mass concentration of the Asian continental aerosol plume from long-term aerosol records in the western United States, *J. Geophys. Res.*, 108(D20), 4623, doi:10.1029/2003JD003459, 2003.

VanCuren, R. A., S. S. Cliff, K. D. Perry, and M. P. Jimenez-Cruz, Continental Aerosol Dominance Above the Marine Boundary Layer in the Eastern North Pacific: Continuous Aerosol Measurements From the 2002 Intercontinental Transport and Chemical Transformation Experiment (ITCT2K2), *J. Geophys. Res.-Atm.*, in press (accepted Feb. 7, 2005).

Walton, J. J., M. C. MacCracken, and S. J. Ghan (1988), "A global-scale Lagrangian trace species model of transport, transformation, and removal processes", *J. Geophys. Res.*, 93, 8339-8354.

Wang, Y., D. J. Jacob, and J. A. Logan (1998), "Global simulation of tropospheric O₃-NO_x-hydrocarbon chemistry: 1. Model formulation", *J. Geophys. Res.*, 103, 10,713-10,725.

Wesely, M. L. (1989), "Improved parameterizations for surface resistance to gaseous dry deposition in regional-scale numerical models", *Atmos. Environ.*, 23, 1293-1304.

Wesely, M. L., D. R. Book, R. L. Hart, and R. E. Speer (1985), "Measurements and parameterization of particulate sulfur dry deposition over grass", *J. Geophys. Res.*, 90, 2131-2143.

Zender, C.S., Miller, R.L., and Tegen, I., "Quantifying Mineral Dust Mass Budgets: Terminology, Constraints, and Current Estimates", *EOS, Transactions, American Geophysical Union*, vol. 85, no. 48, p509, 30 Nov 2004.